Particle Swarm Optimization (PSO) Based MPPT controller Modeling and Design of Photovoltaic Modules

R. A. Muhammed[1*], D. R. Sulaiman[2]
1- Department of Electrical Engineering, Salahaddin University , Erbil, Iraq.
Email: roshna@su.edu.krd (Corresponding author)
2- Department of Electrical Engineering Salahaddin University, Erbil, Iraq.
Email: diary.sulaiman@su.edu.krd

Received: 11 September 2022 Revised: 6 October 2022 Accepted: 27 October 2022

ABSTRACT:
Photovoltaic (PV) panel produces electricity depending on a variety of characteristics, including the PV module model, design specifications, and ambient circumstances such as temperature and sun irradiation. To analyze and model the effect of these factors on PV performance, a PV model is significant to be studied and modeled in advance. It is desirable to be compatible with the real-physical behavior of the PV panel. This paper presents mathematical modeling, design, and simulation of the three-diode model (3DM) MPPT controller instead of using conventional single/double diode PV models. The proposed PV model is analyzed, verified, and simulated at various temperature and irradiance levels. Furthermore, Particle Swarm Optimization (PSO) as a multi-objective algorithm is used for the Maximum Power Point Tracking MPPT controller to enhance the performance of the module and PV array system. A DC/DC boost converter is combined with the proposed 3DM model and connected through a resistive load. Results show that adopting PSO-based MPPT improves the performance of the PV panel compared to the traditional MPPT and verified the theoretical background.

KEYWORDS: Three Diode Model (3DM), Photovoltaic Panel, Particle Swarm Optimization (PSO), Maximum Power Point Tracking (MPPT), Double Diode Model.

1. INTRODUCTION

Green or Renewable Energy Sources (RES) are presently the world's most extensively used source of power since they are clean, free, and ecologically friendly. RES such as photovoltaic (PV) is widely employed to supply the electrical power system [1]. The solar PV array is the most cost-effective common power generator in terms of mechanical installation expenses and running costs [2]. A PV cell or module is equivalent to a P-N junction semiconductor device that converts sunlight energy to electricity [3].

Furthermore, a PV cell can only provide a little amount of DC power; hence, these cells are combined in series to produce a significant output power and are used in conjunction with a PV panel or module [4, 5]. Depending on the production material and commercial maturity, there are various types of PV cell technologies available on the market today. PV cell technologies are classified into three types: polycrystalline, monocrystalline, and thin-film [6]. Polycrystalline cells are inefficient because of the random arrangement of the crystals, and their color is a little blue, reflecting some of the sunlight. While the efficiency of monocrystalline is relatively high [7] because of its uniform dark hue, this technology absorbs a large amount of solar irradiance. As a result, the efficiency of this type is greater than the previous technology but it has certain disadvantages, such as high wafer manufacture costs. Unlike the two previous groups, the thin-film cell type is considered more efficient because it is made from thin layers of amorphous films which results in absorbing more solar irradiance [6]. However, a PV cell or panel has non-linear characteristics since the atmosphere conditions influence the current-voltage (I-V) and power-voltage (P-V) curves of a PV panel [8]. Consequently, a Maximum Power Point Tracking (MPPT) controller is designed to enhance PV output under fluctuating irradiance and ambient temperature conditions [9, 10].

Many types of MPPT controllers were designed and fabricated in recent years. Furthermore, these types may be summarized based on a variety of criteria, including speed response time, cost of implementation, and design complexity [11, 12]. The low-cost perturb and observe (P&O), and incremental conductance (INC) techniques

Paper type: Research paper
DOI: 10.30486/mjee.2023.1970258.0
How to cite this paper: R. A. Muhammed and D. R. Sulaiman, "Particle Swarm Optimization (PSO) Based MPPT controller Modeling and Design of Photovoltaic Modules", Majlesi Journal of Electrical Engineering, Vol. 16, No. 4, pp. 167-175, 2022.

are widely used in PV applications. Although the entire of controllers can provide an acceptable tracking efficiency for the PV module, they have some disadvantages such as high oscillation around the MPP, high power losses, and slow dynamic response [13, 14]. Therefore, an artificial intelligent based MPPT controller like heuristic optimization techniques are essential to enhance the performance and to improve the PV efficiency [15]. A fuzzy logic (FL) based MPPT is used in [15] because its algorithm is a broad approach to express language rules, therefore it can offer a fast answer with basic mathematical non-linear properties and obtains a quick and stable response for the output PV power controller. In addition, to track the MPP of the PV module under various environmental circumstances, a Neural Network (NN) approach is applied in [16]. Genetic algorithm (GA) and Particle Swarm Optimization (PSO) are considered common algorithms used to track and increase the PV module's efficiency [17]. Both algorithms have more advantages and give a very fast dynamic response.

In this paper, PSO based MPPT controller is used as a very fast and more efficient algorithm and applied to control the MSX-60 PV modules in simulations. The single, double, and three PV panel models are analyzed mathematically and then the three-diode model (3DM) for the PV panel is implemented. The proposed 3DM is combined throughout a DC/DC boost converter, and the entire design is simulated. Results are excellent and consistent with the theoretical basics.

2. PHOTOVOLTAIC PANEL MODELS

A PV module is basically a semiconductor diode with a light-exposed P-N junction. In several studies, a single diode circuit model as seen in Fig. (1-A) is used, which is a simple, adequate, and realistic manner of representing the physical behavior of the PV model [18]. In the single diode model, the recombination loss in the depletion zone is neglected. Moreover, the significant losses cannot be precisely predicted. As a result, the physics of a photovoltaic cell is represented by the double–diode model as seen in Fig. (1-B) [19]. Accounting for recombination losses resulted in a more precise model. In this context, the three diode PV model which has three diodes in the PV equivalent circuit seen in Fig. (1-C) can improve the accuracy and make the PV panel's behavior near the reality [20]. Therefore, in this paper, a three-diode PV model is designed and simulated with MPPT controller.

The mathematical equation of the output current for the 3DM (I_pv) can be written as follows [21]:

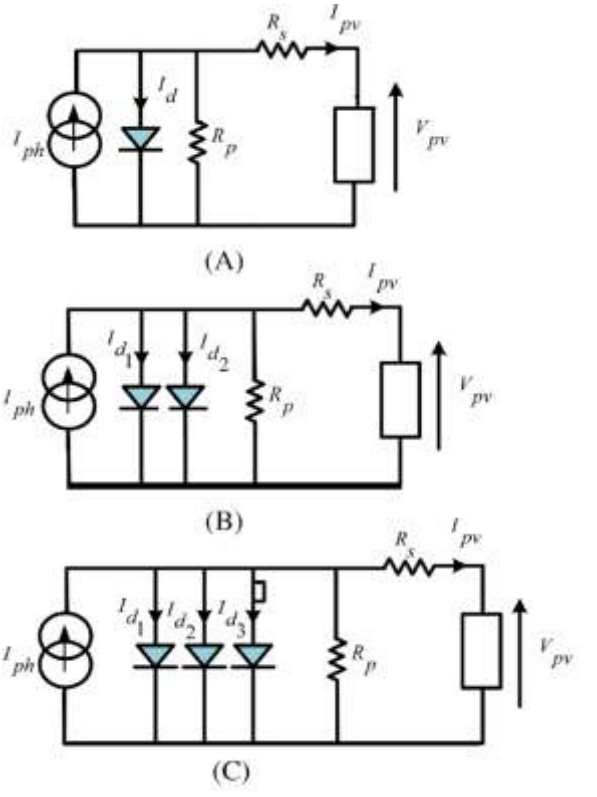

Fig. 1. Single, double, and three diode models for a solar PV panel.

$$I_{pv} = I_{ph} - I_{01}\left\{exp\left[\frac{V_{pv} + I_{pv}\,R_s}{n_1\,V_{th}}\right] - 1\right\} - I_{02}\left\{exp\left[\frac{V_{pv} + I_{pv}\,R_s}{n_2\,V_{th}}\right] - 1\right\} - I_{03}\left\{exp\left[\frac{V_{pv} + I_{pv}\,R_s}{n_3\,V_{th}}\right] - 1\right\} - \frac{V_{pv} + I_{pv}\,R_s}{R_p} \quad (1)$$

The items of Eq. (1) can be defined as follows:

- ✓ I_{ph} represents the photocurrent source.
- ✓ I_{01}, I_{02}, and I_{03} are the saturation diode currents.
- ✓ V_{pv} is the terminal output voltage of a PV model.
- ✓ R_s, R_p are the series and parallel resistance.
- ✓ n_1, n_2, and n_3 represent the diodes ideality factors.
- ✓ V_{th} is the thermal voltage $V_{th} = N_s K\,T/q$.
- ✓ N_s represents the number of cells in a PV panel.
- ✓ K is the Boltzmann constant (1.3806503×10^{-23} J/K).
- ✓ T represents the temperature in Kelvin.
- ✓ q is the electron charge (1.60217646×10^{-19}C).

The saturation and the reverse saturation currents for each diode can be expressed in the equations (2-7) [19, 22].

$$I_{01} = I_{rs1}\left(\frac{T_n}{T}\right)^3 exp\left[\frac{qE_g}{n_1K}\left(\frac{1}{T_n}-\frac{1}{T}\right)\right] \quad (2)$$

$$I_{02} = I_{rs2}\left(\frac{T_n}{T}\right)^3 exp\left[\frac{qE_g}{n_2K}\left(\frac{1}{T_n}-\frac{1}{T}\right)\right] \quad (3)$$

$$I_{03} = I_{rs3}\left(\frac{T_n}{T}\right)^3 exp\left[\frac{qE_g}{n_3K}\left(\frac{1}{T_n}-\frac{1}{T}\right)\right] \quad (4)$$

$$I_{rs1} = \frac{I_{sc}}{\left[\exp\left(\frac{V_{oc}}{n_1V_{th}}\right)-1\right]} \quad (5)$$

$$I_{rs2} = \frac{I_{sc}}{\left[\exp\left(\frac{V_{oc}}{n_2V_{th}}\right)-1\right]} \quad (6)$$

$$I_{rs3} = \frac{I_{sc}}{\left[\exp\left(\frac{V_{oc}}{n_3V_{th}}\right)-1\right]} \quad (7)$$

Where E_g represents the energy of the bandgap ($E_g = 1.12$), T_n is the temperature at STC ($T_n = 298.15\ °K\ or\ 25\ °C$), V_{oc} is the open-circuit voltage and I_{sc} represents the short-circuit current. The photocurrent source is molded using the following equation [18, 23]:

$$I_{ph} = (I_{sc} + K_i\,\Delta T)\frac{G}{G_n} \quad (8)$$

Where, K_i is the coefficient's temperature of the PV current, G represents irradiance and G_n is the irradiance at STC ($G_n = 1000W/m^2$).

3. THREE DIODE PV MODULE USING MATLAB/ SIMULINK TOOL

The primary goal of this paper as mentioned is to use a 3DM to represent a PV module for further accuracy and performance enhancement. The PV panel parameters are extracted from the datasheet at standard test conditions (STC). Table 1 shows the electrical parameters of the used MSX-60W PV panel at STC conditions, and the rest of the parameters for the model R_s, R_p, n_1, n_2, and n_3 are obtained from [20] as seen in Table 2.

Table 1. Datasheet parameters of MSX60W PV panel at STC conditions.

Parameter	Value
Maximum power, P_{mp}	60 W
Maximum voltage, V_{mp}	17.1 V
Maximum current, I_{mp}	3.5 A
Open-circuit voltage, V_{oc}	21.1 V
Short-circuit current, I_{sc}	3.8 A
temperature coefficient at V_{oc}, K_v	$-0.8mV/°C$
temperature coefficient at I_{sc} , K_i	$0.65mA/°C$
Cells of panel N_s	36

Table 2. The rest of MSX-60W PV panel parameters [20].

Parameter	Value
n_1	1.219762
n_2	1.091667
n_3	1.499321
R_s	0.1109557Ω
R_p	349.8458 Ω

Fig. 2 presents the overall PV panel model using 3DM in Matlab/Simulink. The voltage of the PV panel is simulated using ramp function where it is limited as ($0 \le V \le V_{oc}$). Various temperature and irradiance levels are applied to evaluate and test the proposed 3DM. The currents of the 3DM are molded based on their mathematical relations, and the total output current is modeled based on Eq. (1) as shown in the sub-system of Fig. 3.

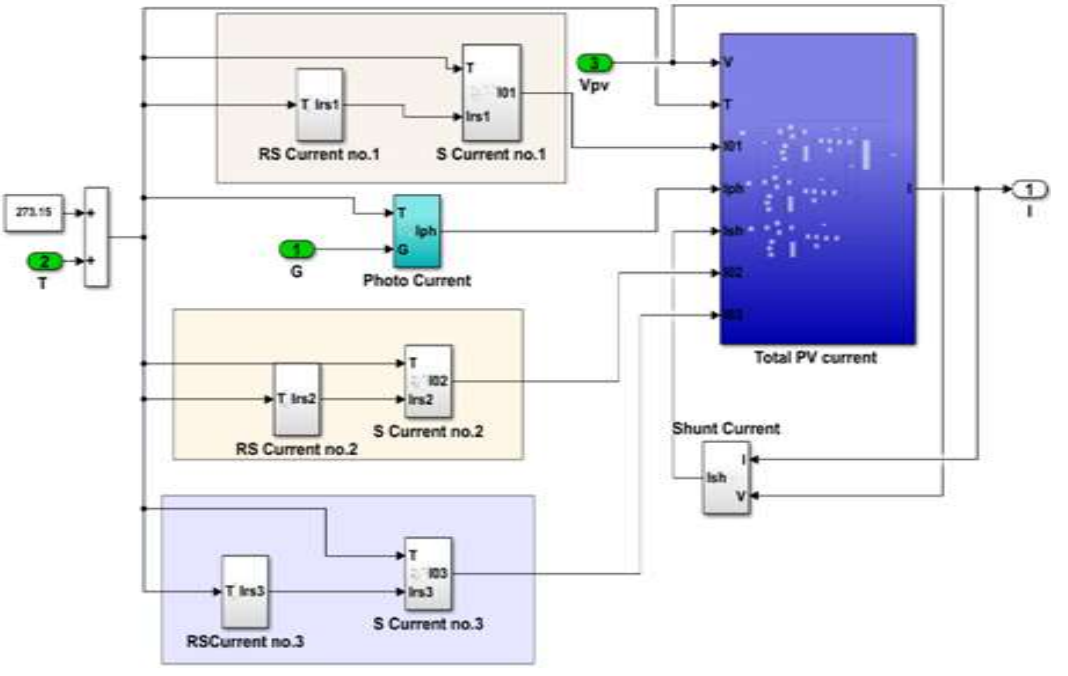

Fig. 2. The MATLAB/Simulink model of a three diode PV module.

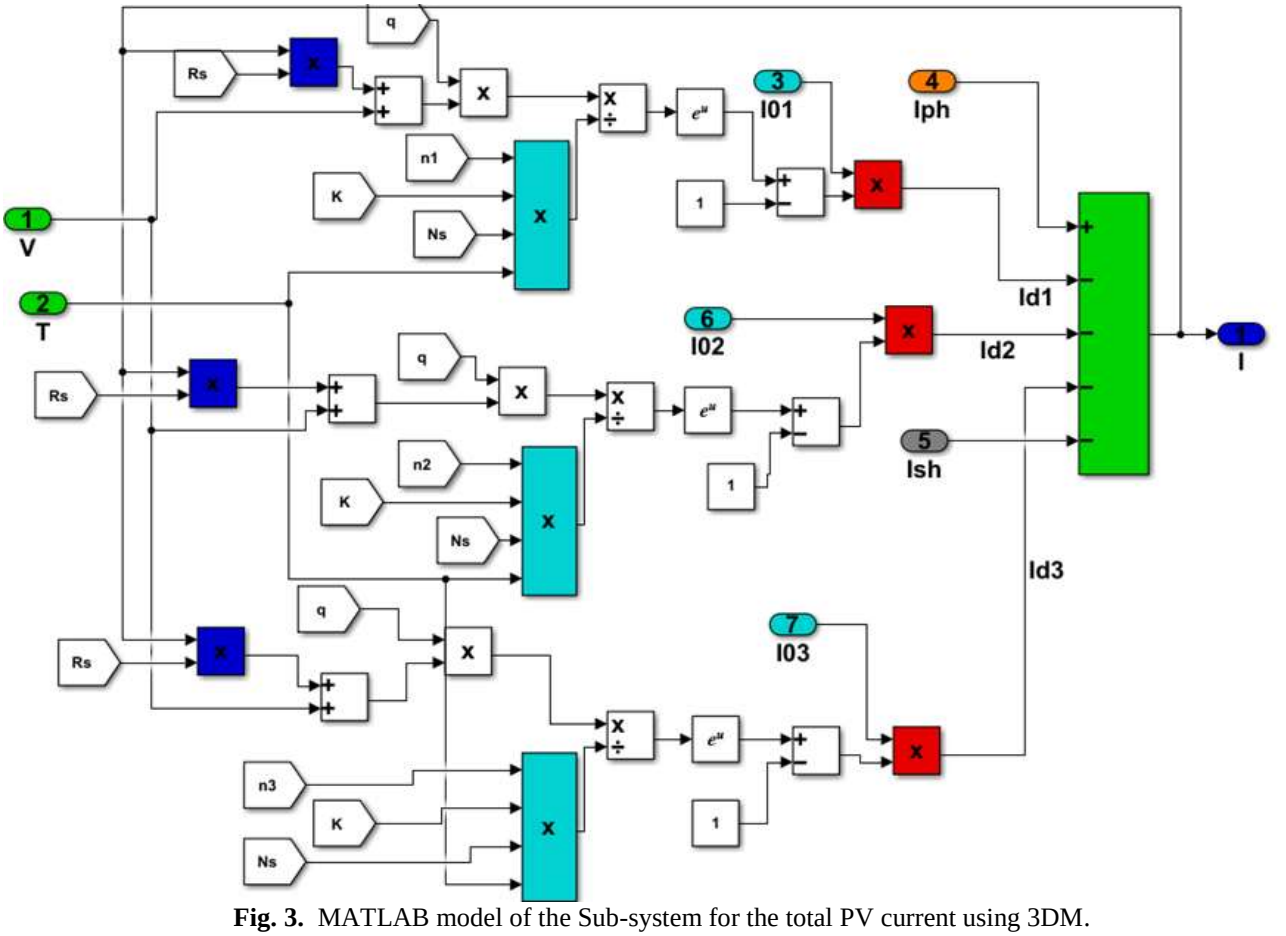

Fig. 3. MATLAB model of the Sub-system for the total PV current using 3DM.

The effectiveness and pertinence of the proposed 3DM PV design are confirmed throughout the simulation steps under various levels of weather conditions. First, the design simulates various irradiance and a fixed temperature $T = 25℃$. The I-V and P-V graphs for the MSX-60W PV are shown in Fig. 4, and the irradiance is varied from 200W/m² to 1000W/m². The curves of the characteristics at 1000W/m² represent the maximum power behavior, while the lower power characteristics are achieved at low irradiances especially at 200W/m². In fact, these variations in curves are occur due to the effect of irradiance on the photocurrent source as indicated in Eq. (8), as the irradiance value decreases, the total current decreases as well, while the change in the temperature is zero ($\Delta T = 0$).

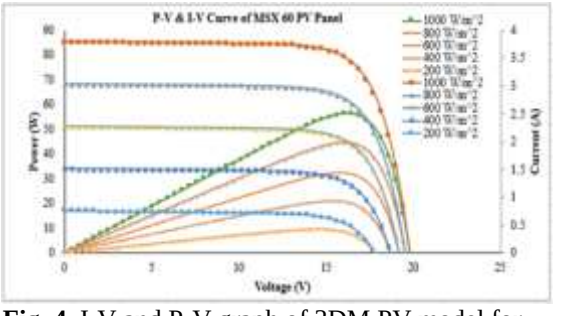

Fig. 4. I-V and P-V graph of 3DM PV model for various irradiance levels and constant temperature.

It is obtained that, the PV panel current is significantly dependent on solar irradiation, as seen in Fig. 4. However, when the level of irradiance is raised from 200W/m² to 1000W/m², the PV panel voltage only increases by 1.5V. Hence, changes in irradiance have a significant impact on the PV panel current.

The influence of temperature fluctuations on the properties of PV panels is seen in Fig. 5. In this case, the suggested model is proven for various temperature levels and constant irradiance ($G = 1000W/m^2$). As shown, with a constant solar irradiation and increasing temperature, the open-circuit voltage drops as the short-circuit current rises with a small amount. As a result, temperature changes have a significant impact on PV panel voltage.

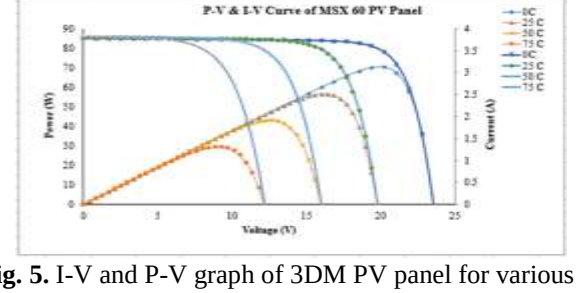

Fig. 5. I-V and P-V graph of 3DM PV panel for various temperature levels and fixed irradiance.

4. MAXIMUM POWER POINT TRACKING CONTROLLER

The purpose of MPPT controllers is to track the PV module's operational point. The MPPT controller is combined with a boost DC/DC converter to modify the duty cycle and match input and output impedances. The accuracy of designing a DC/DC boost converter is considerable and a challenge to implement. The schematic diagram of the MPPT controller for the PV panel and the boost converter used in this paper are presented in Fig. 6. The switching frequency of the converter is set to 5000 Hz and it is designed according to the following parameters:

Cin= 452.5862 uF, Cout= 385.7143 uF, and L= 0.05971mH.

The PSO-based is adopted to the MPPT controller to add further improvements to the design in term of efficiency and the performance.

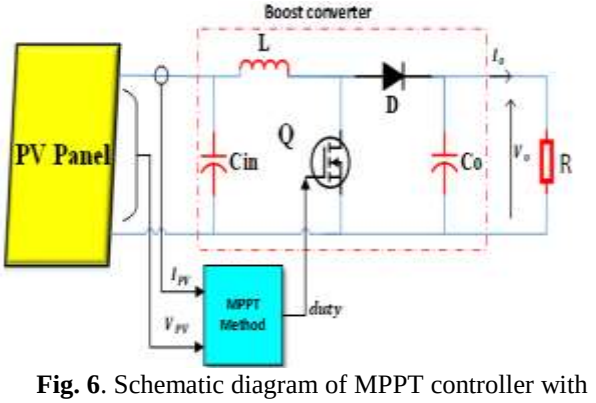

Fig. 6. Schematic diagram of MPPT controller with the PV panel used in this paper.

The Direct control of PSO is used to obtain MPP from the PV system based on the duty ratio with number of particles N^P particles in the swarm. The velocity and position updates in PSO are shown in equations (9-10) [24]:

$$V_i^{m+1} = w \times V_i^m + r_1 \times c_1 \times (P_{bi} - X_i^m) + r_2 \times c_2 \times (G_{bi} - X_i^m) \quad (9)$$

$$X_i^{m+1} = X_i^m + V_i^m \quad (10)$$

Where the parameters of the above equation are defined as follows:

- ✓ i is the optimization vector's variable.
- ✓ m represents the no. of iterations.
- ✓ w represents the factor of inertia.
- ✓ c_1 and c_2 are the coefficients of the

acceleration.

- ✓ r_1 and $r_2 \in U$ (0,1).

X_i^m and V_i^m are the position and velocity of i[th] variable. The best position for a particle P_{bi} is obtained when the equation (11) is satisfied as follows:

$$P_{bi} = X_i^m \;\; If \; F(X_i^m) \geq F(P_{bi}) \qquad (11)$$

The PSO based optimal MPP is achieved when the fitness evaluator F is reached. The PSO based MPPT flowchart is given in Fig. 7. noticeably, when equation (12) is reached, the PSO algorithm has to be initiated.

$$\left|\frac{F(X_{i+1}) - F(X_i)}{F(X_i)}\right| > \Delta P \qquad (12)$$

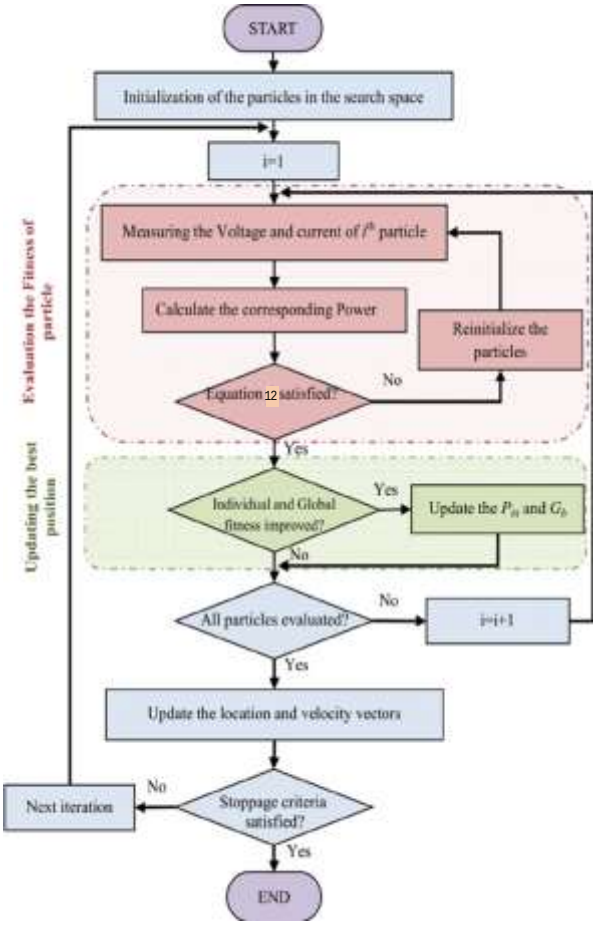

Fig. 7. Algorithm of the PSO based MPPT controller.

5. SIMULATION RESULTS AND TEST THE PERFORMANCE

In order to validate the proposed 3DM PV panel based on PSO MPPT controller, firstly the system is simulated under constant weather conditions (G=1000W/m² and T=25℃), and then at a step change in irradiation while keeping the temperature constant throughout the simulation.

Furthermore, the most used conventional P&O, and INC MPPT techniques are applied on the proposed model. The obtained results are reported in Fig. 8. As depicted, the P&O method presents good speed response and some oscillation around the MPP. This issue repeats in the IC method which produces some power losses. From the comparison, the proposed PSO based MPPT controller added improvements to the system performance with acceptable speed response. As a result, the proposed design improves the system dynamic and the efficiency as well. Fig. 9 shows the simulation results of the PV panel at STC conditions. These results include the PV current, PV voltage and PV power using PSO based MPPT controller. It is clear that, during simulation time t=0.25 second, the obtained curves are sufficient in terms of ripple content, speed dynamic, and oscillation around the MPP at a very short time period at t=0.05 seconds . As shown below, the PV panel's power is near to the maximum power of 60W, which is extracted using the proposed 3DM. Because this model has three current branches, this process causes some recombination losses in the depletion region of the PV panel.

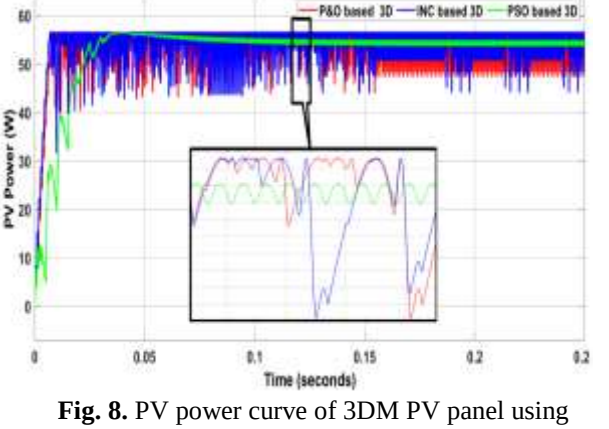

Fig. 8. PV power curve of 3DM PV panel using P&O, INC, and PSO based MPPT techniques at STC condition.

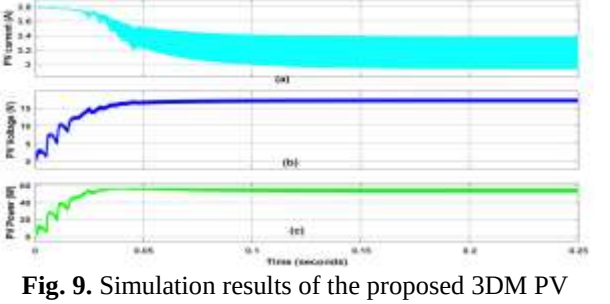

Fig. 9. Simulation results of the proposed 3DM PV model under PSO based MPPT controller at STC condition.

Various irradiance levels are applied to prove the effeteness of the proposed MPPT design. Fig. 10 shows the proposed irradiance profile. Fig. 11 shows the obtained results of PV power using P&O, INC, and PSO methods. As seen in Fig. 11, the PSO method for the MPPT controller offers excellent power oscillation, less ripple content, good dynamic response, and higher efficiency when compared to the other techniques. Also, the INC method suffers when the irradiance increases from low to high and verse versa as this algorithm is based on the idea that the slop of its PV curve is zero at MPP, positive at the left of MPP and negative at the right of MPP, therefore this algorithm is confused when detecting MPP during transient stage, while, the P&O technique is less effect for this manner. The current, voltage, and power of the PV model using PSO based MPPT controller are given in Fig. 12. Consequently, accurate results are obtained using PSO method which proves more stable PV voltage with lower ripple content in case of fast variations of irradiance. The solar irradiance reduces from1000 W/m^2 to 750 W/m^2 at 0.225 s at constant temperature at $T = 25℃$, the PV power reduces from 56.6 W 38.5 W and the current reduces from 3.5 A to 2.6 A, while the voltage reduces from 16.7 V to 14.6 V. Hence, PSO algorithm provides a fast response and settled to the new MPP in short time period when there is a rapid change in irradiation by comparing it to the other methods in terms of both dynamic and steady state response.

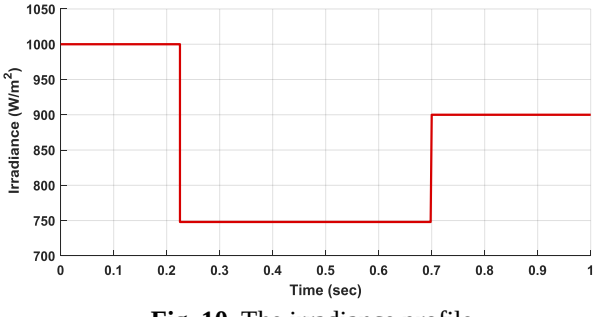

Fig. 10. The irradiance profile.

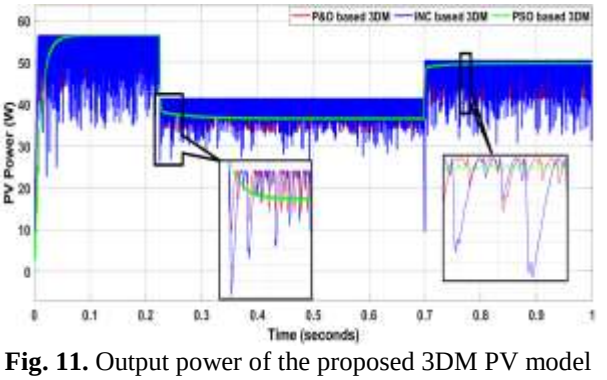

Fig. 11. Output power of the proposed 3DM PV model under P&O, INC, and PSO methods.

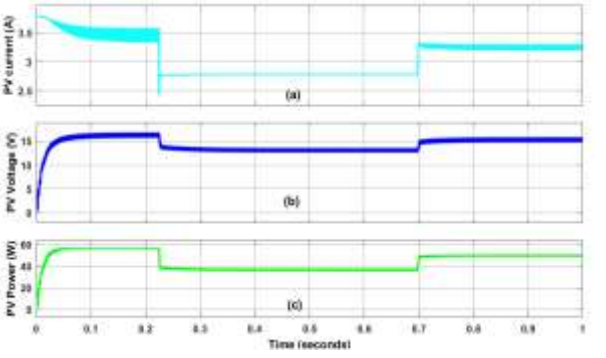

Fig. 12. Simulation results of the PV panel using PSO based MPPT controller.

Table 3 summarizes the simulation results of maximum power in (W) for the three MPPT techniques at a step change of irradiance level from 1000-200 W/m^2 and a fixed temperature as depicted in Fig. 13. It is clear that the maximum power point of PSO method is less than P&O and INC power at low irradiance level. However, PSO method shows less ripple, good speed response, and less oscillation around MPP in comparison with P&O and INC methods as shown in Fig. 8.

Table 3. Simulation Results of MPPT methods at different level of Irradiance.

Irradiance(G) W/m^2	Power		
	PSO	P&O	INC
1000	56.58	56.58	56.58
800	44.57	44.57	44.57
600	26.5	32.68	32.68
400	11.54	20.98	20.98
200	4.38	9.66	9.66

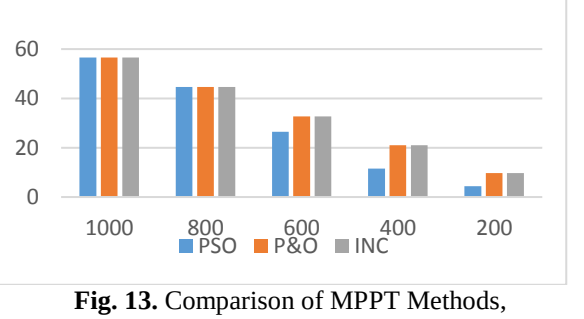

Fig. 13. Comparison of MPPT Methods,

To verify the effectiveness of the three MPPT algorithms in terms of tracking time and power fluctuations, the proposed system is simulated under two different irradiance conditions with a constant temperature ($T = 25℃$) as indicated in Table 4. First, the system is simulated under standard test condition ($G = 1000W/m^2$ and $T = 25℃$), and then under

partially shading condition with the irradiance pattern shown in Fig. 14.

It can be observed from the simulation results that the tracking time for PSO is 0.056 sec when the irradiance is $1000W/m^2$, while it is 0.167 sec and 0.151 sec for P&O and INC respectively at the same irradiance level. In the second case when the system is partially shaded, the tracking time for PSO is also less than the other two algorithms. Furthermore, PSO presents less amount of steady state oscillation compared to P&O and INC algorithms in both irradiance conditions.

Table 4. Comparative Study of MPPT Algorithms.

Irradiance W/m²	MPPT Technique	MPP Power (W)	Tracking Time (Sec)	Steady State Oscillation
Uniform at STC 1000 W/m²	PSO	56.58	0.056	small
	P&O	56.58	0.167	Medium
	INC	56.58	0.151	Large
Partial Shadding	PSO	43.71	0.05	small
	P&O	44.57	0.132	Medium
	INC	44.57	0.126	Large

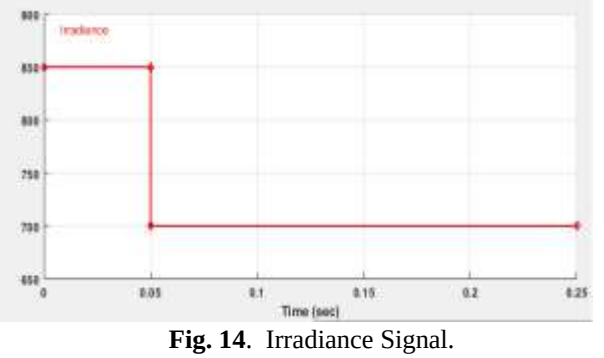

Fig. 14. Irradiance Signal.

6. CONCLUSION

In this paper, the PSO based MPPT controller is imposed on a DC-DC boost converter of a solar PV system under various environmental conditions. The mathematical model of a three-diode model (3DM) for a PV model is presented and simulated under MATLAB/Simulink. The proposed system with PSO based MPPT controller is simulated and compared with P&O and IC algorithms under two different irradiance conditions. Simulation results prove that the PSO based MPPT technique performs better in terms of faster tracking and reduction in output power oscillation which reduces the losses thus increasing the efficiency and improving the performance of the entire system.

It is concluded that, at various weather conditions, the proposed controller is effectively able to track the maximum power faster as compared to the conventional MPPT controller. It is obtained that, using PSO optimization technique has advantages of high precision, high convergence speed, and can effectively track the real maximum power in a photovoltaic system compared to the traditional method.

REFERENCES

[1] Sinsel, S.R., R.L. Riemke, and V.H. Hoffmann, *Challenges and solution technologies for the integration of variable renewable energy sources—a review.* renewable energy, 2020. **145**: p. 2271-2285.

[2] Alonso-García, M. and J. Ruíz, *Analysis and modelling the reverse characteristic of photovoltaic cells.* Solar Energy Materials and Solar Cells, 2006. **90**(7-8): p. 1105-1120.

[3] Dey, B.K., et al. Mathematical modelling and characteristic analysis of Solar PV Cell. in 2016 IEEE 7th Annual Information Technology, Electronics and Mobile Communication Conference (IEMCON). 2016. IEEE.

[4] Nguyen, D.D. and B. Lehman. Modeling and simulation of solar PV arrays under changing illumination conditions. in 2006 IEEE Workshops on Computers in Power Electronics. 2006. IEEE.

[5] Wu, Z., et al., A review for solar panel fire accident prevention in large-scale PV applications. IEEE Access, 2020. **8**: p. 132466-132480.

[6] Nwambaekwe, K.C., et al., Crystal engineering and thin-film deposition strategies towards improving the performance of kesterite photovoltaic cell. Journal of Materials Research and Technology, 2021. **12**: p. 1252-1287.

[7] Ponce-Alcantara, S., C. Del Canizo, and A. Luque, *Adaptation of monocrystalline solar cell process to multicrystalline materials.* Solar energy materials and solar cells, 2005. **87**(1-4): p. 411-421.

[8] Pelap, F., P. Dongo, and A. Kapim, *Optimization of the characteristics of the PV cells using nonlinear electronic components.* Sustainable Energy Technologies and Assessments, 2016. **16**: p. 84-92.

[9] Ali, A., et al., Investigation of MPPT techniques under uniform and non-uniform solar irradiation condition–a retrospection. IEEE Access, 2020. **8**: p. 127368-127392.

[10] Hua, C.-C. and Y.-m. Chen. Modified perturb and observe MPPT with zero oscillation in steady-state for PV systems under partial shaded conditions. in 2017 IEEE Conference on Energy Conversion (CENCON). 2017. IEEE.

[11] Bollipo, R.B., S. Mikkili, and P.K. Bonthagorla, *Hybrid, optimal, intelligent and classical PV MPPT techniques: A review.* CSEE Journal of Power and Energy Systems, 2020. **7**(1): p. 9-33.

[12] Karami, N., N. Moubayed, and R. Outbib, *General review and classification of different MPPT Techniques.* Renewable and Sustainable Energy Reviews, 2017. **68**: p. 1-18.

[13] Motahhir, S., A. El Hammoumi, and A. El Ghzizal, *The most used MPPT algorithms: Review and the suitable low-cost embedded board for each algorithm.* Journal of cleaner production, 2020. **246**: p. 118983.

[14] Christopher, I.W. and R. Ramesh, *Comparative study of P&O and InC MPPT algorithms.* American Journal of Engineering Research (AJER), 2013. **2**(12): p. 402-408.

[15] Nasser, K.W., S.J. Yaqoob, and Z.A. Hassoun, *Improved dynamic performance of photovoltaic panel using fuzzy logic-MPPT algorithm.* Indonesian Journal

of Electrical Engineering and Computer Science, 2021. **21**(2): p. 617-624.
[16] Lin, W.-M., C.-M. Hong, and C.-H. Chen, *Neural-network-based MPPT control of a stand-alone hybrid power generation system.* IEEE transactions on power electronics, 2011. **26**(12): p. 3571-3581.
[17] Ishaque, K., et al., An improved particle swarm optimization (PSO)–based MPPT for PV with reduced steady-state oscillation. IEEE transactions on Power Electronics, 2012. **27**(8): p. 3627-3638.
[18] Shannan, N.M.A.A., N.Z. Yahaya, and B. Singh. Single-diode model and two-diode model of PV modules: A comparison. in 2013 IEEE international conference on control system, computing and engineering. 2013. IEEE.
[19] Yaqoob, S.J., et al., Comparative study with practical validation of photovoltaic monocrystalline module for single and double diode models. Scientific Reports, 2021. **11**(1): p. 1-14.
[20] Elazab, O.S., et al., Parameter estimation of three diode photovoltaic model using grasshopper optimization algorithm. Energies, 2020. **13**(2): p. 497.
[21] Moussa, I. and A. Khedher, Photovoltaic emulator based on PV simulator RT implementation using XSG tools for an FPGA control: Theory and experimentation. International Transactions on Electrical Energy Systems, 2019. **29**(8): p. e12024.
[22] Pandiarajan, N. and R. Muthu, Mathematical modeling of photovoltaic module with Simulink. 2011. 258-263.
[23] Suckow, S., T.M. Pletzer, and H. Kurz, *Fast and reliable calculation of the two‐diode model without simplifications.* Progress in photovoltaics: research and applications, 2014. **22**(4): p. 494-501.
[24] Seyedmahmoudian, M., et al., Maximum power point tracking of partial shaded photovoltaic array using an evolutionary algorithm: A particle swarm optimization technique. Journal of Renewable and Sustainable Energy, 2014. **6**(2): p. 023102.